Exploration of Alternative Models for the Aging of Fouling Deposits

Edward M. Ishiyama, William R. Paterson, and D. Ian Wilson
Dept. of Chemical Engineering and Biotechnology, University of Cambridge, Cambridge CB2 3RA, U.K.

DOI 10.1002/aic.12514
Published online February 9, 2011 in Wiley Online Library (wileyonlinelibrary.com).

*The effect of fouling in heat-transfer devices (HTDs) is complicated by aging of the fouling deposits. Aging is, like deposition, often sensitive to temperature, so that heat transfer, deposition, and aging are coupled phenomena. Ishiyama et al. (*AIChE J. *2010;56:531–545) presented a distributed model of the aging of deposits formed by chemical reaction fouling and illustrated its effect on thermal and hydraulic performance of a HTD operating in the turbulent flow regime. Two-layer models, simpler than the distributed model, are explored. The deposit is considered to consist of two layers, fresh and aged; this simple picture is shown to be sufficient to interpret thermal and hydraulic aspects of deposit aging when HTDs are operated at constant heat flux (as reflecting laboratory experiments) but not in cases where the constant wall temperature approximation is more realistic.* © 2011 American Institute of Chemical Engineers *AIChE J,* 57: 3199–3209, 2011
Keywords: aging, chemical reaction, fouling, modeling

Introduction

Heat-transfer devices (HTDs, e.g., evaporators, boilers, and heat exchangers) often suffer from the problem of "fouling," namely the formation of unwanted deposits on heat-transfer surfaces. Fouling layers can reduce heat-transfer efficiency and process throughput, with associated cost penalties, so fouling mitigation is practiced where feasible. Better understanding of fouling and its implications on process performance is vital in minimizing the penalties resulting from fouling. Epstein[1] classified fouling as being caused by five different mechanisms, introducing a fouling matrix. Moreover, he identified five stages in the formation of fouling layers, common to all mechanisms, namely initiation, transport, adhesion, removal, and aging: the latter refers to the change in the nature of a deposit as it is exposed to conditions in the fouling layer (e.g., higher temperatures as a result of being attached to a hot wall) for an extended period. Yu and Sheikholeslami[2] suggested that the fouling matrix should be extended to incorporate fouling by combined mechanisms. Aging is still an area that requires further understanding, as reported in the latest conference on Heat Exchanger Fouling and Cleaning held in Schladming, Austria.[3] In this article, we consider aging due to extended exposure to hot walls, as arises in crude oil preheat train fouling.[4] Aging can also be caused by other environmental differences, such as cold walls (e.g., with waxes) or dissolved oxygen levels in biofilms.

Aging affects the microstructure of a deposit and, thus, its thermophysical properties. The development of higher solids content and extended order will usually increase the thermal conductivity of a fouling layer, as reported for crystallization fouling by Bohnet et al.[5] The change in structure will also affect the rheology of the layer, usually increasing its cohesion, which affects both fouling (via any removal mechanism) and cleaning (more aggressive chemical or hydraulic conditions will be required to erode it). The reactivity of the material toward cleaning chemicals will also be affected by the chemical and physical changes associated with baking on a solid surface.

Ishiyama et al.[4] presented an analysis of the effects of aging on fouling dynamics, focusing on heat-transfer aspects.

Correspondence concerning this article should be addressed to D. Ian Wilson at diw11@cam.ac.uk.

Table 1. Thermal Conductivity of Carbonaceous Fouling Deposits

Reference	Deposit	Thermal Conductivity ($W\ m^{-1}\ K^{-1}$)
Nelson[6]	Coke flakes	0.07–0.15
Watkinson[7]	Coke-like deposit	0.5–1
Kern[8]	Petroleum coke	5.8 (at 100°C)
Maksimovskii et al.[9]	Coke deposit (from pyrolysis unit)	1–4
Perry and Green[10]	Graphite powder	1.8

Values reported are at 15°C, unless otherwise stated.

The thermal conductivity was assumed to change with time (specifically, to increase, for crude oil fouling layers) at a rate determined by its local temperature; therefore, the thermal conductivity of the deposit varied with position and time. These changes can be considerable, as illustrated by the range in reported thermal conductivity values in Table 1.

The phenomenon of aging is well established in the crude oil fouling literature. The aging of HTD deposits was discussed by Nelson,[6] who described the formation of cokes (carbonaceous fouling layers) in the vaporization of oil at the tube wall at high furnace temperatures. Coke formation was described as arising from chemical reactions in the film of liquid at the wall; its adverse effect on heat transfer was detailed. The properties of the layer would change with temperature and time, essentially by baking.

Atkins[11] considered fouling in furnaces and in the hottest exchangers in a crude oil preheat train and proposed that the formation of the hard coke fouling layer occurred via two steps, namely the deposition of a porous coke or tarry layer, which was then converted to a hard coke layer. The transition from the tarry or porous layer to the hard coke was modeled as a phase change, occurring at a fixed temperature, so that the growth of a hard coke followed a moving front. Crittenden and Kolaczkowski[12] extended the Atkins two-layer concept, which they modeled as

$$\text{Precursors (in bulk fluid)} \xrightarrow[\text{net deposition}]{} \text{tarry foulant layer} \xrightarrow[\text{aging}]{} \text{coke}$$

They proposed a quantitative description of the evolution of the overall fouling resistance, in which the changing thicknesses of the tarry layer and its conversion to the coke layer were evaluated. The growth of tarry layer was described as a competition between deposition, mass transfer of tarry components back into the bulk solution, and shear removal of the tarry layer. They compared the trends predicted by their model with chemical reaction fouling data reported by Watkinson and Epstein,[13] where the deposit was described as "soot-like," so they were not able to explore the coke formation regime.

Aging has received considerable attention in relation to wax deposition in undersea oil pipelines.[14-18] Aging there causes hardening of the deposits and makes their removal difficult. Numerical modeling of the aging process in waxes has included analyses based on thermodynamics (crystallization from solution) in combination with transport dominated by mass transfer and by heat transfer.[19]

Understanding the evolution of the structure of fouling deposits due to aging and the impact on further fouling requires a detailed model such as that proposed by Ishiyama et al.,[4] which was extended to spatially distributed systems such as heat exchanger tubes by Coletti et al.[20] The change in structure caused by aging is likely to be distributed monotonically within the deposit (from aged to fresh material) because there is unlikely to be much mixing within a static, stratified foulant, and diffusion will be slow.

In many food, water and chemical applications the fouling deposit undergoes an aging transformation over the lifetime of the run, from its initial, freshly-deposited form to a more cohesive material. In this case, the extent of aging determines the state of the layer and, therefore, the ease with which a fouling layer can be removed. The effectiveness of a cleaning method would require attention as described by Ishiyama et al.[21]

This article revisits the modeling of aging deposits where chemical reaction is the major mechanism for deposition. A simpler two-layer concept to represent deposit aging is introduced in the variants. The concept is similar to that proposed by Atkins and is believed to have computational merit, being simple to incorporate into heat exchanger simulation codes. Illustrations are given for a point in a tube with crude oil flowing on the tube side at a constant mass flow rate. The bulk liquid flow is in the turbulent regime. On the tube side, a deposit is developed, which is subjected to aging. Over time, changes in the thermal and hydraulic resistances caused by fouling are computed, with a view, (1) to compare the prediction of the two-layer models with the distributed model and (2) to compare different modes of operation, namely at constant wall temperature and constant heat flux. Point (2) is of practical importance as laboratory data are often obtained via constant heat flux operation, whereas industrial heat exchangers approximate constant wall temperature operation. The treatment focuses on the thermal impact of fouling, as the film heat-transfer coefficients are relatively large, and the presence of an insulating layer on the wall has a significant effect on the rate of heat transfer (compared with the hydraulic effect resulting from deposit thickness).

Model Formulation: Aging and Deposition Models

Aging of a deposit, associated with the transition from an initial material into a harder, usually more conductive material, may be modeled as being (1) gradual and continuous (distributed models) or (2) locally complete (two-layer models). The difference between these is shown in Figure 1. The terms "gel" and "coke," often applied to crude oil deposits, are used to label the terminal states, although the models may well be applicable to systems other than crude oil. In the two-layer model, part of the initial gel is completely converted to coke, the thickness of the coke layer growing gradually with time, as a moving front (Path I). In contrast, the distributed model involves a gradual transition from the soft, gel-like material to the hard, coke-like material (Path II); as the structure of the deposit changes, so does its thermal conductivity: this happens at different rates at different points in the deposit. The scope for using the two-layer model to describe real behavior is investigated here using a one-dimensional representation.

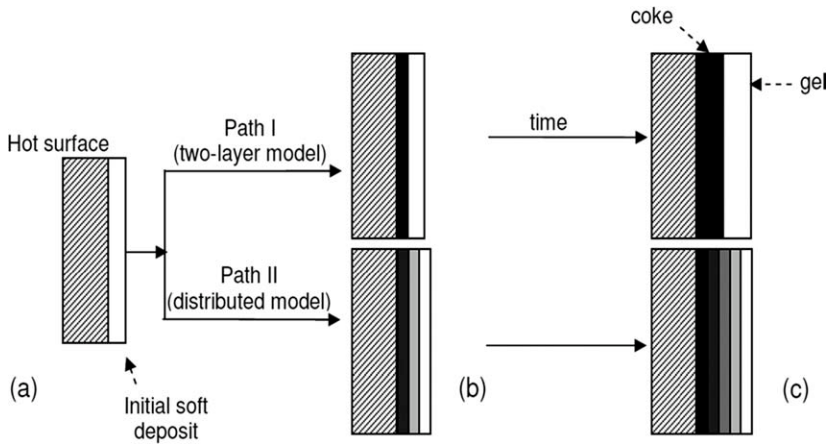

Figure 1. Schematic comparison of two-layer and distributed aging models.

The deposit changes from its initial soft form (a) to a harder, aged form as the layer grows (b, c). Darkness of shading indicates the degree of aging.

A shell-and-tube heat exchanger is considered where a fluid prone to fouling (e.g., crude oil) flows through the tubes and a nonfouling stream flows on the shell side. Fouling deposits are therefore formed only on the tube side. Axial distribution of deposit thickness, and other variables, is not considered.

In the two-layer model, the thermal conductivity of the coke is higher than that of the gel. Similarly, in the distributed model, the thermal conductivity of the deposit increases with the degree of aging (conversion to coke). For convenience, and because of a lack of experimental data, the densities of the gel and coke material are assumed to be equal, i.e., aging of the deposit does not influence its thickness.

The same deposition rate model is used in the different aging models. For purposes of comparison, the chemical reaction fouling model used by Ishiyama et al.[4] is used here to evaluate the rate of foulant deposition, r_d, given as cubic meter of deposit formed per meter square of deposit surface per second

$$r_d = \lambda_{gel} a_d Re^{-0.8} Pr^{-0.33} \exp\left(\frac{-E_d}{RT_s}\right) \tag{1}$$

Here, Re and Pr are the Reynolds number and Prandtl numbers of the bulk liquid, respectively; T_s is the temperature at the surface of the deposit, i.e., in contact with the flowing fluid, R is the gas constant, E_d is the activation energy for deposition, and a_d is a pre-exponential factor dictating the time scale of deposition. λ_{gel} is the thermal conductivity of the gel. In this article, a single value of E_d is used, namely 50 kJ mol^{-1}, which is representative of temperature sensitivities reported for industrial systems,[22] except for the case of $E_d = 0$ in the bilinear model that is described in section "Bilinear Model (Model III)." Different activation energies are considered for the aging step, so that the effect of temperature sensitivity on aging can be isolated from its effect on deposition.

The model (Eq. 1) was developed for crude oils undergoing heating with (liquid) flow in the turbulent regime. Re and Pr are given by

$$Re = \frac{\rho u_m (d_{inner} - 2\delta)}{\mu} \tag{2}$$

$$Pr = \frac{C_p \mu}{\lambda_b} \tag{3}$$

Here, C_p, ρ, μ, and λ_b are the specific heat capacity, density, dynamic viscosity, and thermal conductivity of the fluid flowing through the tube at bulk temperature; u_m is the mean axial velocity; d_{inner} is the internal diameter of the tube; and δ is the deposit thickness. For the case study considered here, the Reynolds and Prandtl numbers for the bulk flow were ~40,000 and ~9.5, respectively.

In evaluating T_s, a value for the tube-side film heat-transfer coefficient, h_{inner}, is required, which is estimated using the Gnielinski correlation[23]

$$h_{inner} = \left(\frac{\lambda_b}{d_{inner} - 2\delta}\right) \frac{\left(\frac{C_f}{2}\right)(Re - 1000)Pr}{1 + 12.7\sqrt{\frac{C_f}{2}}(Pr^{0.67} - 1)} \tag{4}$$

where C_f is the Fanning friction factor. The Fanning friction factor, C_f, is in turn dependent on surface roughness, e, and flow velocity, as described by the Colebrook–White equation.[24] An explicit form of this relationship is given by Sousa et al.[25]

$$\frac{1}{\sqrt{C_f}} = -4\log_{10}\left(\frac{e}{3.7(d_{inner} - 2\delta)} - \frac{5.16}{Re}\log_{10}\left(\frac{e}{3.7(d_{inner} - 2\delta)} - \frac{5.09}{Re^{0.87}}\right)\right) \tag{5}$$

Two-layer model

The two-layer approach as proposed by Crittenden and Kolaczkowski[12] is not used here because of its complexity; instead, a two-layer model inspired by their concept is introduced.

The overall fouling thermal resistance, R_f, is calculated as the sum of the resistances of the gel and the coke layers, using the thin-slab approximation

$$R_f = \frac{\delta_{gel}}{\lambda_{gel}} + \frac{\delta_{coke}}{\lambda_{coke}} \quad (6)$$

Here, λ_j and δ_j are the thermal conductivity and the thickness, respectively, of the relevant layer. Subscripts "gel" and "coke" refer to the gel and coke deposits, respectively.

The thin-slab approximation is used to simplify the heat-transfer calculations without introducing unreasonable errors (as described by Yeap et al.,[22] curvature effects would have to be included for a thick deposit, $\delta/d_{inner} > \sim 0.15$). Still, to capture the effect of deposition on the hydraulic performance, deposit thickness is included in the pressure drop calculations.

The total thickness of the deposit, δ, is calculated from

$$\delta = \delta_{gel} + \delta_{coke} \quad (7)$$

The rates of change of the thickness of the two layers are given by

$$\dot{\delta}_{gel} = r_d - r_c \quad (8)$$

$$\dot{\delta}_{coke} = r_c \quad (9)$$

where r_c is the rate of conversion of gel to coke (cubic meter of coke formed per meter square of gel–coke surface per second). The overall thermal fouling rate, $\dot{R}_f$, is then given by

$$\dot{R}_f = \frac{1}{\lambda_{gel}}(r_d - r_c) + \frac{1}{\lambda_{coke}} r_c \quad (10)$$

Evaluation of r_c is subject to debate. Two different approaches are compared here: assuming (1) zeroth-order reaction or (2) first-order reaction (in terms of the thickness of gel present).

There is a temperature distribution for the two-layer model as implied in Figure 2. The interface temperatures are calculated through solving the heat balance equations

$$Q = \left(\frac{\lambda_{coke}}{\delta_{coke}}\right) A_1 (T_{wall} - T_{int}) \quad (11)$$

$$Q = \left(\frac{\lambda_{gel}}{\delta_{gel}}\right) A_2 (T_{int} - T_s) \quad (12)$$

$$Q = h_{inner} A_3 (T_s - T_b) \quad (13)$$

where Q is the heat duty, T_{wall} is the tube-wall temperature, T_{int} is the coke–gel interface temperature, T_s is the deposit-fluid interface temperature, and T_b is the bulk fluid temperature. A_j (where $j = 1, 2, 3$) is the respective heat-transfer surface area. When the unit is operated at constant wall temperature, T_{wall} and T_b are known; for constant heat flux operation, Q/A_1 and T_b are known. Calculations of δ_{coke} and δ_{gel} will be detailed with the formulation of the two-layer model.

In both of the approaches, T_{int} is treated as a constant during a time interval from t_{n-1} to t_n and then reevaluated at t_n.

Simple Euler integrations are used in this study. The rate of deposition is the factor that determines the accuracy of the numerical result. The deposition rate of the case study is that of a typical crude oil, where the Euler integration method was shown to be sufficient, accurate, and fast by Ishiyama et al.[26] The focus in this work was to test the feasibility of the two-layer concept, for which the numerical platform takes secondary importance. The numerical methodologies could be improved in future work (such as the use of Runge–Kutta methods).

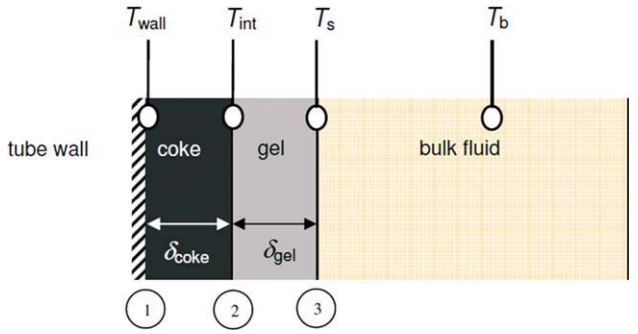

Figure 2. Schematic of the interface temperatures based on the two-layer model.

T_{wall}, T_{int}, T_s, and T_b are the tube-wall, coke–gel layer interface, gel-bulk fluid interface, and the fluid bulk temperatures, respectively. [Color figure can be viewed in the online issue, which is available at wileyonlinelibrary.com.]

r_c Zeroth Order (Model 0)

In this analysis, r_c is given by

$$r_c = \begin{cases} k_0 & \text{when } \delta_{gel} > 0 \\ 0 & \text{when } \delta_{gel} = 0 \end{cases} \quad (14)$$

and

$$k_0 = a_0 \exp\left(\frac{-E_0}{RT_{int}}\right) \quad (15)$$

Here, k_0 is a rate constant, T_{int} is the gel–coke interface temperature, a_0 is the pre-exponential factor, and E_0 is the activation energy for aging. The discontinuity in Eq. 14 arises from there being no aging in the absence of a deposit.

Deposition of the fresh fouling layer and its subsequent aging are evaluated separately at each time step.

The thickness of the gel layer at the time instant t_n, δ_{gel,t_n}, is deduced by substituting (14) and (15) into (8) and (9) and integrating

$$\delta_{gel,t_n} = \delta_{gel,t_{n-1}} + r_d \Delta t - a_0 \exp\left(\frac{-E_0}{RT_{int}}\right)\Delta t, \ \delta_{gel} > 0 \quad (16)$$

Here, $\delta_{gel,t_{n-1}}$ is the gel thickness at the time instant t_{n-1}.

Similarly, the coke layer thickness at time instant t_n is given by

$$\delta_{coke,t_n} = \delta_{coke,t_{n-1}} + a_0 \exp\left(\frac{-E_0}{RT_{int}}\right)\Delta t, \ \delta_{gel} > 0 \quad (17)$$

r_c First Order (Model I)

In this model, self-deterioration is imposed on the rate of conversion of gel to coke by having it depend on the thickness of gel present via a first-order relationship

$$r_c = k_I\ \delta_{gel} = a_I \exp\left(\frac{-E_I}{RT_{int}}\right)\delta_{gel} \tag{18}$$

Here, k_I is the rate constant for conversion and δ_{gel} is the total thickness of the gel layer; a_I is the pre-exponential factor and E_I is the activation energy for aging. It could be argued that aging is an interfacial phenomenon and that it would be physically implausible for the rate of coke formation to depend directly on the thickness of gel present. Nevertheless, this mathematical formulation is introduced here to establish how this simple-minded first-order kinetic model compares with the behavior of the first-order distributed model reported under section "r_c First Order (Model I)."

There would be no aging of the deposit in the absence of a deposit; hence, the deposition of the foulant and its subsequent aging are evaluated separately at each time step.

Deposition and aging are considered separately in the time interval Δt; the gel layer is assumed to undergo a first-order decay, and so the thickness of the gel layer at time instant t_n is given by

$$\delta_{gel,t_n} = \left[r_d \Delta t + \delta_{gel,t_{n-1}}\right] \exp\left(-a_I \exp\left(\frac{-E_I}{RT_{int}}\right)\Delta t\right) \tag{19}$$

Similarly, the thickness of the coke layer is given by

$$\delta_{coke,t_n} = \delta_{coke,t_{n-1}} + \left(\delta_{gel,t_{n-1}} - \left[r_d \Delta t + \delta_{gel,t_{n-1}}\right] \exp\left(-a_I \exp\left(\frac{-E_I}{RT_{int}}\right)\Delta t\right)\right) \tag{20}$$

Bilinear Model (Model III)

For comparison purposes later in this article, consider a case where both the net rate of gel formation and the net rate of coke formation are independent of temperature, i.e., the case of the zeroth-order model with $E_0 = E_d = 0$. This is considered the simplest possible form of the two-layer model, where the rate of coke formation and gel formation are constant.

Distributed Aging Model (Model IV)

Ishiyama et al.[4] presented a distributed aging model for aging occurring on a point of a heat-transfer surface, which is summarized below. Conceptually, the deposit is continuous. It is, however, computed by discretization as sublayers, laid down at fixed time steps to form a series of annuli with varying history (Figure 3). Once deposited, each sublayer is covered by the next sublayer, with deposition occurring only at the deposit-liquid interface. The thickness of the ith sublayer is denoted δ_i and does not change with time, being determined by the conditions at its formation. The thermal conductivity of the ith sublayer, denoted $\lambda_{f,i}$, however, increases with time as the sublayer ages. Formulations for evaluating the interface temperatures between the sublayers, T_i, are detailed in Ref. 4.

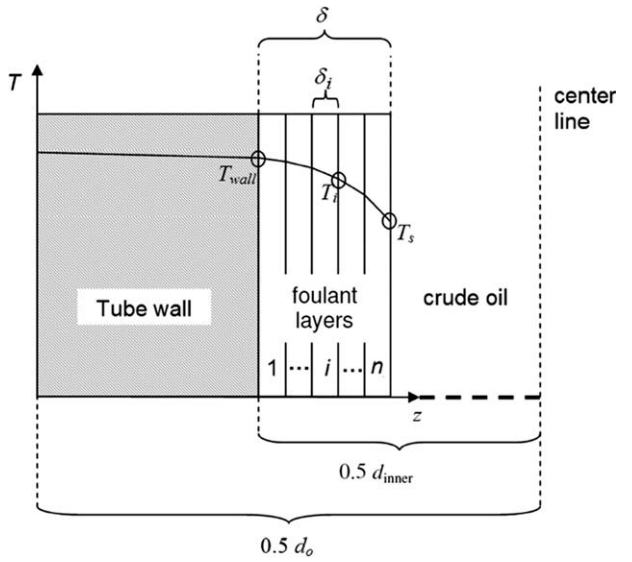

Figure 3. Schematic of distributed aging model for fouling in a heat exchanger tube.

Axis T represents the temperature and z is the distance from the outer surface of the tube, measured toward the tube center line. Foulant layers are labeled from 1 to n, with n marking fresh deposit at the layer/oil interface. d_{inner} is the tube internal diameter, d_o is the tube external diameter, T_{wall} is the wall temperature, T_i is the surface temperature of the ith layer (facing the center line), and T_s is the deposit/oil interface temperature. Reproduced from Ishiyama *et al.*[4]

The upper limit of thermal conductivity, i.e., for fully coked material, is denoted as λ_{coke}, whereas the freshly deposited foulant always has a thermal conductivity, λ_{gel}, corresponding to the lower bound of the observed range, say 0.2 W m^{-1} K^{-1}. For a given surface condition, the thickness of each sublayer, δ_i, is calculated from

$$\delta_i = \left.\frac{d\delta}{dt}\right|_i \Delta t = r_{d,t_i} \Delta t \tag{21}$$

where $\left.\frac{d\delta}{dt}\right|_i$ is the local rate of deposit growth at time period i and Δt the time step over which the deposit forms. The overall fouling resistance, R_f, after m layers have been formed, is estimated as a series of resistances

$$R_f = \sum_{i=1}^{m} \frac{\delta_i}{\lambda_{f,i}} \tag{22}$$

and the total deposit thickness, δ, at time $t = m\Delta t$

$$\delta = \sum_{i=1}^{m} \delta_i \tag{23}$$

The thermal conductivity of each sublayer at time instant t, $\lambda^t_{f,i}$, varies between the limiting values $\{\lambda_{gel}, \lambda_{coke}\}$ according to

$$\lambda^t_{f,i} = \lambda_{coke} + \left[\lambda_{gel} - \lambda_{coke}\right] \cdot y^t_i \tag{24}$$

where y^t_i is named the "youth" variable

$$0 \leq y_i^t \leq 1 \tag{25}$$

The youth variable is postulated to decline from its initial value of $y_i^0 = 1$ according to a first-order kinetic scheme, viz

$$\frac{dy_i^t}{dt} = -k_{II,i}^t y_i^t \tag{26}$$

Here, $k_{II,i}^t$ is an aging rate constant and follows an Arrhenius dependency on temperature

$$k_{II,i}^t = a_{II} \exp\left(\frac{-E_{II}}{RT_{i,d}}\right) \tag{27}$$

where $T_{i,d}$ is the arithmetic average temperature of the ith sublayer, a_{III} is the pre-exponential factor, which defines the absolute rate of decay, and E_{II} is the activation energy of aging (determining its temperature dependency). The rate of change of thermal conductivity of each layer is, therefore, dependent on the local temperature, via

$$\Delta \ln y_i^{t_{n-1}} = \left[-a_{II} \exp\left(\frac{-E_{II}}{RT_{i,d}}\right)\right]\Delta t \tag{28}$$

where $T_{i,d}$ varies with position and time.

Basis for Comparing Aging Models

Thermal performance

Only thermal measurements (i.e., temperature data) are readily available, in many practical situations, such as in the operation of preheat trains in crude oil refineries. It is important to build a framework through which the models presented in section "Model Formulation: Aging and Deposition Models" could be compared based on thermal fouling behavior. The main objective of the comparison is to identify whether the simplified two-layer model could be used to represent the more sophisticated distributed model. In cases where two-layer models could be used, a major computational benefit is expected in terms of incorporating the aging model with the existing fouling models.

In this article, the thermal effects of aging are compared for fouling on the tube side of a shell-and-tube heat exchanger. The thermal effect of deposition and aging is quantified in terms of the overall thermal resistance, expressed in dimensionless form via the fouling Biot number, Bi_f, defined as

$$Bi_f = R_f \; h_{inner,cl} \tag{29}$$

Here, $h_{inner,cl}$ is the tube-side film heat-transfer coefficient of the equipment at clean state. R_f is determined using Eq. 6 in the case of the two-layer models and Eq. 22 for the distributed model.

A dimensionless time, t^*, is introduced. This is the ratio between the operating time of a particular HTD to the characteristic fouling time, t_c

$$t^* = t/t_c \tag{30}$$

The characteristic fouling time, t_c, for a particular unit is the time taken for its Biot fouling number to reach 1, when operated under constant mass flow. For the constant heat flux operation, t_c is 152 days, and for the constant wall temperature operation t_c is 274 days.

In the analysis, two operating modes will be considered: (1) operation at constant heat flux, q, and (2) operation at constant wall temperature, T_{wall}. Laboratory test rigs often operate in the former mode, whereas the latter often offers a closer approximation to industrial heat exchanger operation. It is worth pointing out that both the heating and the cooling fluids could foul on a single HTD, in which case neither the constant wall temperature nor the constant heat flux operation modes would be directly applicable.

Hydraulic performance

Deposition results in reduction of cross-sectional area for flow and in the worst case, tube blockage (clogging). Tube blockage (as could be exhibited in certain industrial shell-and-tube exchangers) is not discussed in the case study, as modeling this phenomenon requires understanding of the flow distributions through partially blocked and unblocked tubes, which is not within the scope of this work. Considering the deposit surface to be smooth, the hydraulic effect is quantified in terms of the pressure drop across a tube subject to fouling, expressed as a dimensionless pressure drop ratio[22]

$$\frac{\Delta P}{\Delta P_{cl}} = \left(1 - \frac{2\delta}{d_{inner}}\right)^{-5} \tag{31}$$

Here, ΔP is the pressure drop for the fouled equipment, ΔP_{cl} is the pressure drop at the clean state, d_{inner} is the internal diameter of the tube, and δ is the thickness of the fouling layer. As the thickness of the deposit layer is assumed not to be affected by aging, the hydraulic effect provides an indication, albeit a nonlinear one, of deposit growth.

Rates of aging

In the earlier article by Ishiyama et al.,[4] a range of different aging rates were explored keeping the same initial fouling rate. The deposition rate model parameters a_d and E_d determine the layer thickness. The distributed aging model parameters a_{II} and E_{II} determine the subsequent change in the layer thermal conductivity, and the two phenomena together determine the surface temperature and subsequent rate of deposition, and aging. Deposition and aging therefore interact, with a ratio of characteristic frequency factors, $\psi = a_{II}/a_d^*$, where $a_d^* = a_d Re^{-0.8} Pr^{-0.33}$ and temperature dependencies related to the difference in activation energies, $\Delta E = E_d - E_{II}$.

The initial value of a_d^* is set at 10 m^2 K $kW^{-1}h^{-1}$, giving an initial fouling rate in the illustrations of 4.2×10^{-11} m^2 K J^{-1}, which lies in the range of fouling rates reported for shell-and-tube exchangers operated at the hot end of a preheat train with bulk oil temperatures above 200 °C.[27] The range of ratios of frequency factors, ψ, reported by Ishiyama et al.[4] were used, which were set to 0.1, 1.0, and 10 (W m^{-2} K^{-1}), termed slow, medium, and fast aging, respectively.

Table 2. Parameters Used in Aging and Deposition Models

			$E_0 = E_I = E_{II}$	
			10 kJ mol^{-1}	200 kJ mol^{-1}
Two-layer model	Zeroth order a_0 (day^{-1})	Slow	3.53×10^{-6}	0.20×10^{13}
		Medium	6.00×10^{-6}	0.85×10^{13}
		Fast	6.45×10^{-6}	1.2×10^{13}
Two-layer model	First order a_I (day^{-1})	Slow	0.06	5.6×10^{16}
		Medium	0.40	7.0×10^{17}
		Fast	0.85	3.4×10^{18}
Distributed model	a_{II} (day^{-1})	Slow	0.024	4.48×10^{16}
		Medium	0.24	4.48×10^{17}
		Fast	2.40	4.48×10^{18}

Deposition model parameters, $a_d = 1 \times 10^5$ m^2 K kW^{-1} h^{-1}, $E_d = 50$ kJ mol^{-1}.

For each ratio, the effect of temperature sensitivity was explored by comparing E_{III} values of 10 kJ mol^{-1} ($\Delta E > 0$) and 200 kJ mol^{-1} ($\Delta E < 0$). Also, to provide a consistent basis for comparison, the initial aging rate was held constant by compensating a_{II} for the change in E_{II} via

$$a_{II,E\ II} = a_{II,10\ kJ\ mol^{-1}} \exp\left(-\frac{10,000 - E_{II}}{RT_s}\right) \tag{32}$$

If such compensation had not been introduced, the effect of increasing E_{II} alone would merely have been to slow the aging rate; with compensation, the effect of increasing sensitivity of aging rate to temperature can be studied.

The impact of different magnitudes of the parameters ψ and ΔE was investigated by Ishiyama et al.[4] based on values representative of those obtained from crude oil fouling measurements. Similar parameters for the distributed model were used here and are listed in Table 2. The physical properties of the fluid and the operational parameters used in the simulation are listed in Table 3.

The parameters for the two-layer models, a_I and a_{II} (Table 2), were determined for $E_0 = E_I = E_{II}$, with a_0 and a_I selected such that these gave the same Bi_f value as the distributed model at the end of a 250-day simulation, for constant heat flux operation. The 250-day period was that used by Ishiyama et al.,[4] but is otherwise an arbitrary selection. The same parameter values used in the constant heat flux operation were used for the constant wall temperature operation.

Different operating modes

The heat-transfer equations used in performing constant wall temperature and constant heat flux calculations are detailed in Ref. 4.

For operation at constant wall temperature, the value of T_{wall} was set at 270°C, being representative of the hot end of a typical crude oil refinery preheat train. For operation at constant heat flux, the value of q was selected to give the same initial surface temperature (270°C) as in the constant wall temperature operation case.

Results and Discussion

Constant heat flux

For constant heat flux operation, the temperature of the deposit and fluid interface remains constant, so the deposition rate (following Eq. 1) remains constant. The rate of aging does not, therefore, affect the rate of deposition, i.e., the effects of aging and deposition are decoupled.

In constant heat flux operation, aging affects the temperature distribution within the deposit strongly. The heat flux, q, is related to the temperature difference across the deposit by the overall fouling resistance via

$$q = h_{inner}(T_s - T_b) = \frac{1}{R_f}(T_{wall} - T_s) \tag{33}$$

Maintaining q, h_{inner}, and T_b constant forces T_s to be constant. At the start of a test, when no deposit is present, $T_{wall} = T_s$. Rearranging Eq. 33

$$T_{wall} = T_s + R_f q \tag{34}$$

It should be noted that the above analysis is the basis of measuring R_f used in many experimental fouling studies. The temperature within the deposit will therefore increase over time, and aging, as described by the kinetic model presented here, will be accelerated. Equation 33 can also be written as

$$\begin{aligned} T_{wall} - T_s &= Bi_f(T_s - T_b) \\ \frac{T_{wall} - T_s}{T_s - T_b} &= Bi_f \end{aligned} \tag{35}$$

reinforcing the impact of fouling on temperatures in the deposit.

Table 3. Physical Properties and Operating Parameters Used in the Simulations

Parameter	Value	Reference
d_{inner}	0.0229 m	Sinnott et al.[28]
d_o	0.0254 m (1 inch, Gauge 18)	
Mass flow rate	0.3 kg s^{-1}	
Specific heat capacity (J kg^{-1} K^{-1})	$C_p = 1787.5 + 5.0433T_b$	Ishiyama et al.[4]
Density (kg m^{-3})	$\rho = 877.02 - 0.8379T_b$	
Dynamic viscosity (mPa s)	$\mu = 1498.7{T_b}^{-1.5611}$	
Thermal conductivity (W m^{-1} K^{-1})	$\lambda = 0.1367 - 0.00009T_b$	

T_b is the fluid bulk temperature in °C. For this example, Re and Pr at 270°C are ~40,000 and ~9.5, respectively.

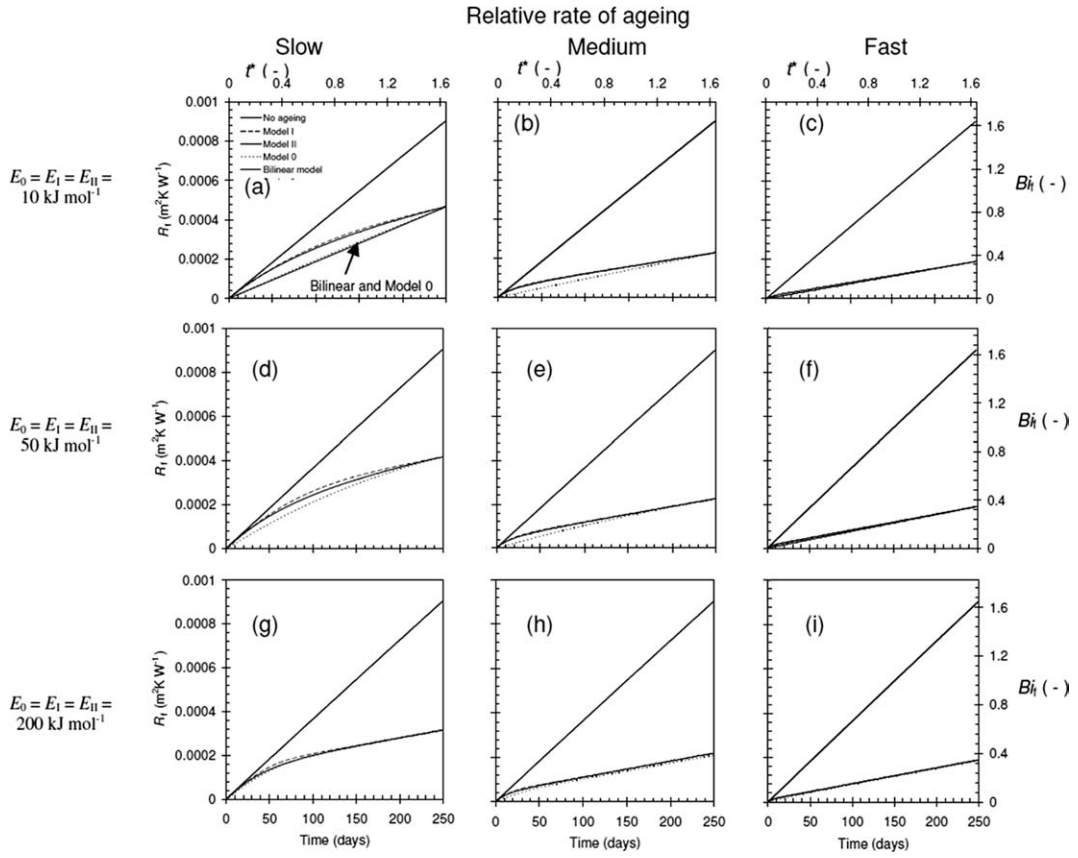

Figure 4. Comparison of aging models under constant heat flux operation.

Key in (a) common to all plots. Model 0—two-layer, zeroth order; Model I—two-layer, first order; Model II—distributed model. The bilinear model is illustrated in (a) only.

The results for the different cases are summarized in Figure 4 (secondary axes represent the dimensionless parameters t^* and Bi_f). The effect of aging on thermal behavior is evident, as discussed by Ishiayama et al.[4] Comparing the different models in Figure 4, it can be seen that the net rate of aging predicted by the distributed model (gray solid line) proves to be mimicked well by the first-order two-layer model (dashed line) in all cases. The zeroth-order two-layer model gives better agreement with the distributed model at higher values of E_i and when aging is fast.

The bilinear model and the two-layer zeroth-order model agree with each other when E_i is 10 kJ mol^{-1} (Figures 4a–c) and when the rate of aging is fast (Figures 4c, f, i). The bilinear model gives poor agreement with the distributed and first-order two-layer models at $E_i = 10$ and 50 kJ mol^{-1} as it does not contain any temperature sensitivity; similarly, all three temperature-sensitive aging models deviate from the bilinear model at high E_i.

When the rate of aging is fast, any deposit formed is quickly converted to coke. Thus, the transition period from gel to coke is short, trending in the limit toward the two-layer models. Hence, all four aging models tend to agree under conditions of fast aging.

As the deposition rate remains constant for constant heat flux operation, the final value of $\Delta P/\Delta P_{cl}$ for the different aging rates remains the same. The two extreme cases of Bi_f against $\Delta P/\Delta P_{cl}$ behavior are plotted in Figure 5, where Figure 5a corresponds to slow aging with an activation energy for aging of 10 kJ mol^{-1} and Figure 5b considers fast aging with an aging activation energy of 200 kJ mol^{-1}. Aging then manifests itself in differences in thermal behavior only. It should be noted that the deposit thickness is linear with time and so could substitute for the time scale. The pressure drop ratio, moreover, given by $\Delta P/\Delta P_{cl}$ is nonlinear with time according to Eq. 30, but for small values of thickness it could be approximated as linear.

Table 4 gives a summary of how the two-layer models match the distributed model over these investigations. Overall, Model I (first-order two-layer model) gave good agreement with the distributed model, whereas Model 0 (the zeroth-order form) gave a reasonable representation only for a high aging activation energy (200 kJ mol^{-1}) or for fast aging, where the distributed model necessarily approximates growth of the coke layer as a moving front. When the distributed model is a good approximation to the experiments, experiments yielding thermal measurements could be interpreted using Model I with some confidence, and Model 0 only where there was evidence of fast aging or of the aging mechanism involving a highly temperature-sensitive step.

Constant wall temperature

When a unit is operated at constant wall temperature, the deposit temperature always lies between the wall temperature and the bulk fluid temperature. As the deposit grows the

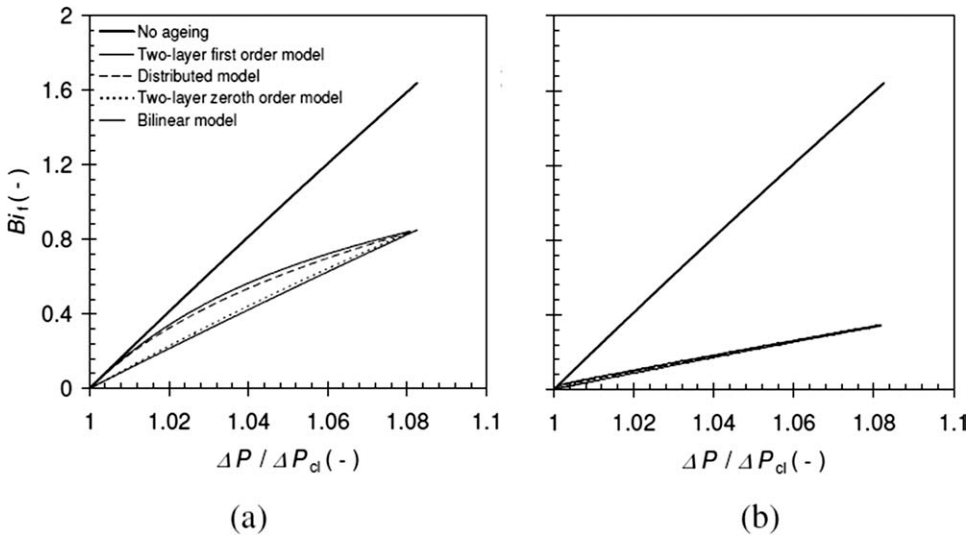

Figure 5. Bi_f against $\Delta P/\Delta P_{cl}$.

(a) 10 kJ mol^{-1}, slow aging and (b) 200 kJ mol^{-1}, fast aging, constant heat flux.

surface temperature decreases, decreasing the rate of deposit formation. Deposit formation is no longer linear with time as was the case in constant heat flux operation.

The different combinations of aging rate and aging activation energy were simulated under conditions of constant wall temperature, using the same parameters as the constant heat flux case. In this case, however, the deposition and aging phenomena are intrinsically coupled. The results are summarized in Figure 6 (secondary axes represent the dimensionless parameters t^* and Bi_f), which shows that the four aging models do not usually agree with each other, and neither of the two-layer models is consistently superior in terms of matching the distributed model.

The two-layer first-order model is superior to the zeroth-order form for an aging activation energy of 10 kJ mol^{-1} (Figures 6a–c) but at higher activation energies the agreement is poor, particularly at longer times. The zeroth-order model gives better agreement under some cases, but this is not systematic (moving from Figures 6a, d, g; b, e, h; c, f, i).

Table 5 summarizes when the zeroth- and first-order two-layer models could be used to represent the distributed model. Neither model agrees well with the distributed model over all situations considered. The two-layer concept shows limitations compared with the distributed model, which is a cost associated with introducing the computational simplifications.

Comparison of constant heat flux and constant wall temperature operations

The results in Figure 4 show that it would be difficult to differentiate the two-layer models on the basis of thermal fouling resistance data obtained under constant heat flux conditions except in the initial stages of fouling or where the aging step was not sensitive to temperature. Figure 6, however, shows that the two models exhibit noticeably different behaviors for the constant wall temperature scenario. Consider, for example, Figure 4i, showing constant heat flux operation where the two-layer models match the distributed model well. Figure 6i shows the same aging model parameters used for a constant wall temperature mode, where the two-layer models both deviate from the distributed model. At day 100, the fouling resistance obtained from the zeroth-order two-layer model is ~40% greater than that of the distributed model.

Many laboratory studies are performed using constant heat flux, as this often affords constant deposition rates. This investigation shows that caution must be used in selecting a two-layer aging model (either zeroth and first order) to describe the thermal fouling data obtained from such studies if aging is suspected to be significant, particularly if the models are to be used in turn to simulate the operation of devices operating at constant wall temperature (such as some boilers, condensers, and evaporators). If the distributed model is taken to give a more accurate representation of the aging process, the most appropriate two-layer model to use can be seen to depend on the rate and temperature sensitivity of the aging process. Where there is uncertainty about the nature or extent of aging, further experimental evidence will be required. Another view of this same phenomenon would be that experiments performed at constant wall temperature have greater power to discriminate between different aging models than experiments performed at constant heat flux. This latter point does require the effect of surface temperature on the deposition rate (e.g., Eq. 1) to be known, preferably by separate measurements.

Table 4. Summary of Relative Agreement of the Two-Layer Models (Model 0—Zeroth-Order Model and Model I—First-Order Model) with the Distributed Model for Constant Heat Flux Operation

	Relative Rate of Aging		
	Slow	Medium	Fast
$E_0 = E_I = E_{II} = 10$ kJ mol^{-1}	Model I	Model I	Both
$E_0 = E_I = E_{II} = 50$ kJ mol^{-1}	Model I	Model I	Both
$E_0 = E_I = E_{II} = 200$ kJ mol^{-1}	Both	Both	Both

Entry indicates good agreement.

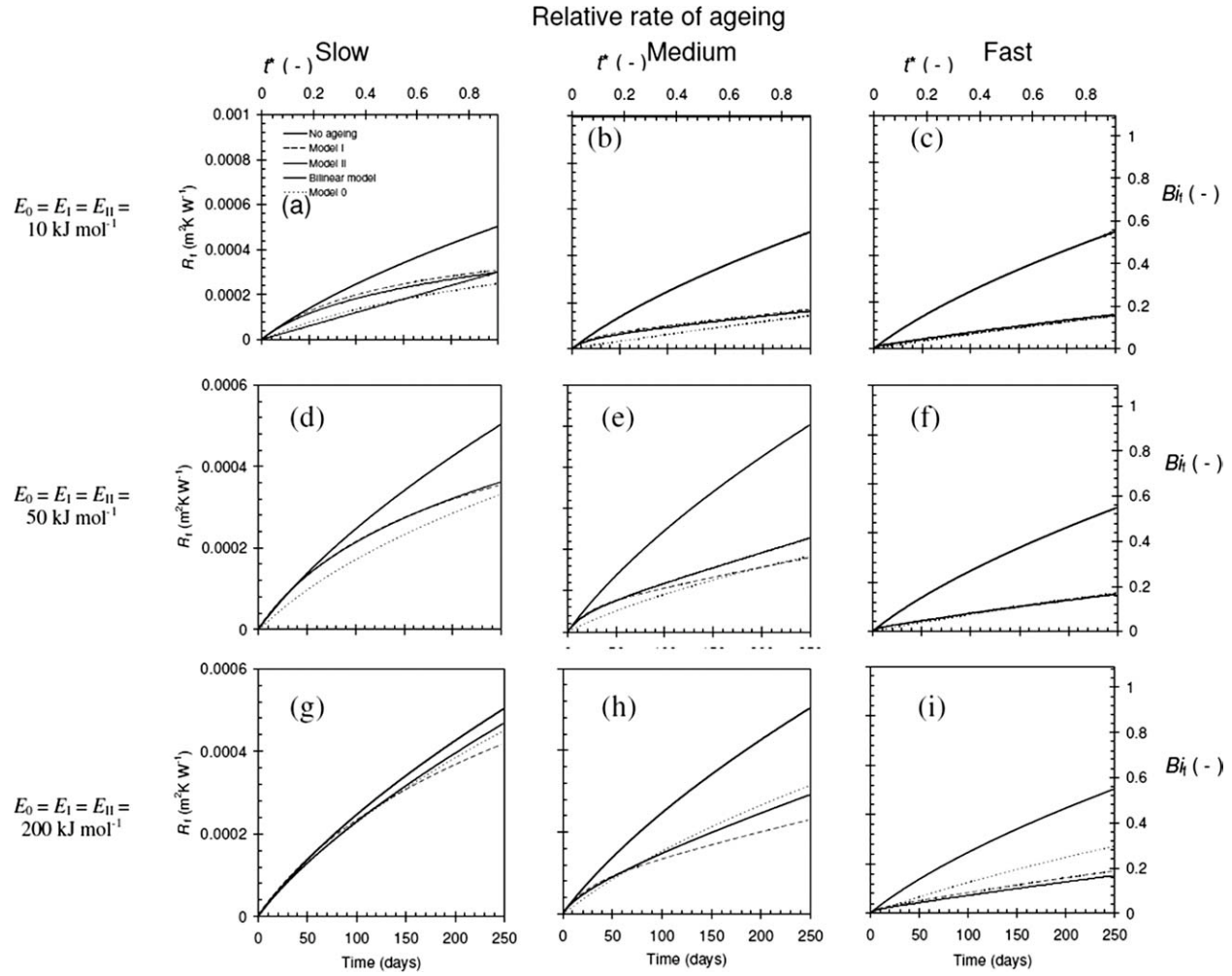

Figure 6. Comparison of aging models under constant wall temperature operation.

Key in (a) common to all plots. Model 0—two-layer, zeroth order; Model I—two-layer, first order; Model II—distributed model. The bilinear model is illustrated in (a) only.

Conclusions

The thermal and hydraulic implications of deposit aging predicted by three simple two-layer models (zeroth order, first order, and bilinear) were compared with a more sophisticated distributed aging model. When deposit aging follows an Arrhenius temperature dependency, the first-order two-layer model was shown to give reasonable agreement with the distributed model, particularly for calculations made at constant heat flux. This agreement no longer holds when the unit is operated at constant wall temperature.

Table 5. Summary of Relative Agreement of the Two-Layer Models (Model 0—Zeroth-Order Model and Model I—First-Order Model) with the Distributed Model for Constant Wall Temperature Operation

	Relative Rate of Aging		
	Slow	Medium	Fast
$E_0 = E_I = E_{II} = 10$ kJ mol^{-1}	Model I	Model I	Both
$E_0 = E_I = E_{II} = 50$ kJ mol^{-1}	Model I	Neither	Both
$E_0 = E_I = E_{II} = 200$ kJ mol^{-1}	Neither	Neither	Neither

Entry indicates good agreement.

The above points show that care must be taken when using these simplified two-layer aging models to describe laboratory experiments, i.e., in fitting experimental R_f time data sets to one of the models in order to extract model parameters, or to confirm aging effects. Particular care is needed if a model is to be used for prediction of a process or unit operated at constant wall temperature if the model parameters were obtained from experiments performed using constant heat flux. Tables 4 and 5 indicate when one of the models provides more reliable agreement with the distributed model, and this should be used to guide the choice of model if both were to give good descriptions of the observed aging behavior.

Even though the first-order two-layer model agrees well with the distributed model, there is no physical evidence that the aging process is first order. In terms of physical reasoning, the zeroth-order model is more attractive as it attributes aging to a surface phenomenon. Further modeling would gain from experimental evidence.

Notation

a_0 = pre-exponential term in Eq. 15 (m s^{-1})
a_I = pre-exponential term in Eq. 18 (s^{-1})
a_{II} = pre-exponential term in Eq. 28 (s^{-1})
a_d = pre-exponential term in Eq. 1 (m^2 K J^{-1})
a_d* = lumped pre-exponential term (m^2 K J^{-1})
A = heat-transfer area (m^2)
Bi_f = fouling Biot number
C_f = Fanning friction factor
C_p = specific heat capacity (J kg^{-1} K^{-1})
d = tube diameter (m)
e = surface roughness (m)
E_0 = activation energy in Eq. 15 (kJ mol^{-1})
E_I = activation energy in Eq. 18 (kJ mol^{-1})
E_{II} = activation energy in Eq. 28 (kJ mol^{-1})
E_d = activation energy in Eq. 1 (kJ mol^{-1})
h = film heat-transfer coefficient (W m^{-2} K^{-1})
k_0 = kinetic parameter in Eq. 15 (m s^{-1})
k_I = kinetic parameter in Eq. 18 (s^{-1})
k_{II} = kinetic parameter in Eq. 26 (s^{-1})
ΔP = pressure drop (N m^{-2})
Pr = Prandtl number
Q = heat duty (W)
q = heat flux (W m^{-2})
R = gas constant (kJ mol^{-1} K^{-1})
R_f = fouling resistance (m^2 K W^{-1})
$\dot{R}_f$ = rate of fouling (m^2 K J^{-1})
r_c = rate of coke formation (m s^{-1})
r_d = net rate of deposition (m s^{-1})
Re = Reynolds number
t = time (s, day)
t_c = characteristic time (s)
t* = dimensionless time
T = temperature (K)
u_m = mean axial velocity (m s^{-1})
y = youth variable

Greek letters

δ = deposit thickness (m)
$\dot{\delta}$ = rate of deposit growth (m s^{-1})
λ = thermal conductivity (W m^{-1} K^{-1})
μ = dynamic viscosity (Pa s)
ρ = density (kg m^{-3})
ψ = characteristic frequency factor (W m^{-2} K^{-1})

Subscripts

b = fluid bulk
cl = clean state
coke = coke layer
d = deposit
f = foulant layer
gel = gel layer
i = ith layer
inner = tube internal
int = at the interface
o = tube external
s = surface
t_n = at time instant t_n
t_{n-1} = at time instant t_{n-1}
wall = at the tube wall

Superscript

t = at time t

Literature Cited

1. Epstein N. Thinking about heat transfer fouling: a 5 × 5 matrix. *Heat Transfer Eng*. 1983;4:43–56.
2. Yu H, Sheikholeslami R. Composite fouling on heat exchange surface in Australian sugar mill evaporator. *Heat Transfer Eng*. 2009;30:1033–1040.
3. Mueller-Steinhagen H, Watkinson AP, Wilson DI. Preface. 2009. Available at: http://heatexchanger-fouling.com/proceedings2009.htm.
4. Ishiyama EM, Coletti F, Macchietto S, Paterson WR, Wilson DI. Impact of deposit ageing on thermal fouling: lumped parameter model. *AIChE J*. 2010;56:531–545.
5. Bohnet N, Augustin W, Hirsch H. Influence of fouling layer shear strength on removal. Editors, LF Melo, CB Panchal, EFC Somerscales. In: *Understanding Heat Exchanger Fouling and Its Mitigation*. New York: Begell House, 1999:201–208.
6. Nelson W. Fouling of heat exchangers. *Refiner Nat Gas Manuf*. 1934;13:271–276, 292–298.
7. Watkinson AP. Critical review of organic fluid fouling. Final Report, ANL/CNSV-TN-208, Argonne National Laboratory, 1988:136.
8. Kern DQ. *Process Heat Transfer*. McGraw-Hill Companies, Singapore. 1988.
9. Maksimovskii V, Raud É, Sokolov O, Korsak I, Chepovskii M. Thermal conductivity of coke deposited in quenching-evaporative equipment of pyrolysis units. *Chem Technol Fuels Oils*. 1990;26:584–587.
10. Perry RH, Green DW. *Perry's Chemical Engineers' Handbook*. McGraw-Hill, Sydney, Australia. 2007:6–10.
11. Atkins GT. What to do about high coking rates. *Petro/Chem Eng*. 1962;34:20–25.
12. Crittenden BD, Kolaczkowski ST, PW O'Callaghan. Energy savings through the accurate prediction of heat transfer fouling resistances. In: *Energy for Industry*. London: Pergamon Press, 1979:257–266.
13. Watkinson AP, Epstein N. Gas oil fouling in a sensible heat exchanger. *Chem Eng Prog Symp Ser*. 1969;65:84–90.
14. Singh P, Venkatesan R, Fogler HS, Nagarajan N. Formation and aging of incipient thin film wax-oil gels. *AIChE J*. 2000;46:1059–1074.
15. Singh P, Youyen A, Fogler HS. Existence of a critical carbon number in the aging of a wax-oil gel. *AIChE J*. 2001;47:2111–2124.
16. Singh P, Venkatesan R, Fogler HS, Nagarajan NR. Morphological evolution of thick wax deposits during aging. *AIChE J*. 2001;47:6–18.
17. Paso KG, Fogler HS. Influence of n-paraffin composition on the aging of wax-oil gel deposits. *AIChE J*. 2003;49:3241–3252.
18. Paso KG, Fogler HS. Bulk stabilization in wax deposition systems. *Energy Fuels*. 2004;18:1005–1013.
19. Bidmus HO, Mehrotra AK. Solids deposition during "cold-flow" of wax solvent mixtures in a flow loop apparatus with heat transfer. *Energy Fuels*. 2009;6:3184–3194.
20. Coletti F, Ishiyama EM, Paterson WR, Wilson DI, Macchietto S. Impact of deposit ageing and surface roughness on thermal fouling: distributed model. *AIChE J*. 2010;56:3257–3273.
21. Ishiyama EM, Paterson WR, Wilson DI. The effect of ageing of fouling-cleaning symbiosis. In: *Conference Proceedings of the International Conference on Fouling and Cleaning in Food Processing*, Cambridge, UK, 2010:128–135.
22. Yeap BL, Wilson DI, Polley GT, Pugh SJ. Mitigation of crude oil refinery heat exchanger fouling through retrofits based on thermo-hydraulic fouling models. *Chem Eng Res Des*. 2004;82:53–71.
23. Gnielinski V. New equations for heat and mass transfer in turbulent pipe and channel flow. *Int Chem Eng*. 1976;16:359–368.
24. Colebrook C, White C. Fluid friction in roughened pipes. *Proc R Soc London Ser A*. 1937;161:367–381.
25. Sousa J, da Conceicao Cunha M, Sa Marques A. An explicit solution to the Colebrook-White equation through simulated annealing. In: Savic DA, Walters GA, editors. *Water Industry Systems: Modelling and Optimization Applications*. UK: Research Studies Press Ltd., 1999:347–355.
26. Ishiyama EM, Paterson WR, Wilson DI. Platform for techno-economic analysis of fouling mitigation options in refinery preheat trains. *Energy Fuels*. 2009:23:1323–1337.
27. Ishiyama EM, Paterson WR, Wilson DI, Heins AV, Spinelli L. Scheduling cleaning in a crude oil preheat train subject to fouling: incorporating desalter control. *Appl Therm Eng*. 2010;30:1852–1862.
28. Sinnott RK, Coulson JM, Richardson JF. *Chemical Engineering Design*. Butterworth-Heinemann, Oxford, United Kingdom. 2005: 634–668.

Manuscript received Jun. 25, 2010, and revision received Nov. 3, 2010.